http://dx.doi.org/10.5935/0103-5053.20130276

J. Braz. Chem. Soc., Vol. 25, No. 1, 112-118, 2014.
Printed in Brazil - ©2014 Sociedade Brasileira de Química
0103 - 5053 $6.00+0.00

Article

Structural Study and Fluorescent Property of a Novel Organic Microporous Crystalline Material

Zhao Cheng, Bingqin Yang,* Meipan Yang and Binglin Zhang

Key Laboratory of Synthetic and Natural Functional Molecule Chemistry of Ministry of Education, College of Chemistry and Materials Science, Northwest University, 710069 Xi'an, China

Um novo material orgânico microporoso [(2-{2-[2-(bis-metoxicarbonilmetilamino)fenoxi] etoxi}-4-benzimidazol-fenil)metoxicarbonilmetilamino] éster metílico do ácido acético **6** foi sintetizado e caracterizado por difração de raio X de cristal único, espectroscopia no infravermelho por transformada de Fourier (FT-IR), espectrometria de massas de alta resolução com ionização por electrospray (ESI-HRMS), difração de pó (PXRD) e RMN do ^{1}H e ^{13}C. **6** cristaliza em grupos de espaço monoclínico centrossimétrico *C*2/*c*, com parâmetros de célula unitária *a* = 35,648(3) Å, *b* = 14,3240(12) Å, *c* = 15,3693(13) Å, α = 90,00, β = 94,8190(10), γ = 90,00, V = 7820,16 Å^3 e *Z* = 8 a 296(2) K. Conforme indicado pelo empacotamento cristalino, os planos de conjugação molecular se organizam ao longo do eixo *c* para formar microporos devido às ligações de hidrogênio. Além disso, espectro de fluorescência e tempo de vida de luminescência foram estudados para **6**.

A novel microporous organic material [(2-{2-[2-(bis-methoxycarbonylmethylamino)phenoxy] ethoxy}-4-benzimidazole-phenyl)methoxycarbonylmethylamino]acetic acid methyl ester **6** was synthesized and characterized by single crystal X-ray diffraction, Fourier transform infrared spectroscopy (FT-IR), electron spray ionization-mass spectrometry (ESI-HRMS), X-ray powder diffraction (PXRD), ^{1}H and ^{13}C NMR. **6** crystallizes in the centrosymmetric monoclinic space group *C*2/*c*, with unit cell parameters *a* = 35.648(3) Å, *b* = 14.3240(12) Å, *c* = 15.3693(13) Å, α = 90.00, β = 94.8190(10), γ = 90.00, V = 7820.16 Å^3 and *Z* = 8 at 296(2) K. As indicated by crystal packing, the molecular conjugation planes arrange along the *c* axis to form micropores due to the hydrogen bonds. In addition, the fluorescent spectrum and luminescence lifetime were studied for **6**.

Keywords: X-ray diffraction, hydrogen bond, microporosity, fluorescence, luminescence lifetime

Introduction

During recent years, research on porous organic crystalline materials is of particular interest for their broad application in chemical separating,[1] capturing,[2] and gas storing.[3] Many recent studies have focused on the most successful application: the gas storage. In this field, some measures that aim to obtain an improved performance of microporous materials are adopted, such as optimizing pore size and surface area.[4,5] However, other functions of microporous materials excluding gas storage have not been well studied. This motivated us to explore microporous materials with novel properties. Herein, a novel luminescent organic microporous crystalline material [(2-{2-[2-(bis-methoxycarbonylmethylamino)phenoxy]ethoxy}-4-benzimidazole-phenyl)methoxycarbonylmethylamino] acetic acid methyl ester **6** is reported. This structure contains benzene and imidazole functionalities to enhance luminescence and shows the property to form microporous skeleton via intramolecular[6-8] and intermolecular hydrogen bonds (Figure 1).[8,9]

Benzimidazoles have been widely used in chromatography.[10-13] Most studies are associated with the spectroscopic and structural properties of benzimidazole[14,15] and some of its derivatives coordination compounds containing benzimidazole group[16]. In general, free imidazole molecule does not have visible light absorption.[17-19] To improve the photoabsorption properties of imidazole, it is possible to introduce some groups with conjugated structures, such as benzene.

The single crystal X-ray structural study, as an efficient method to reveal molecular conformation, intra- and

*e-mail: yangbq@nwu.edu.cn

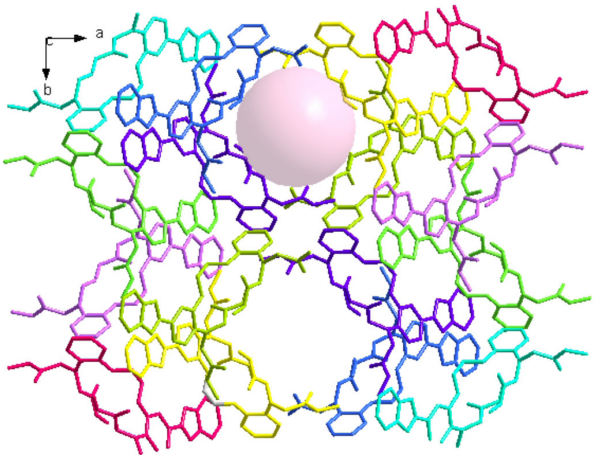

Figure 1. Schematic representation of void cage in **6** with V_{void} of 20% (total potential solvent occupied volume of 1563.1 Å^3 *per* unit cell volume). The molecular skeleton with same color located at centrosymmetric position.

intermolecular interactions in solid state of substances, can help us better understand and refine molecular structures in order to optimize certain properties.

Herein, structural and spectroscopic studies of a novel microporous crystalline material [(2-{2-[2-(bis-methoxycarbonylmethylamino)phenoxy]ethoxy}-4-benzimidazole-phenyl)methoxycarbonylmethylamino] acetic acid methyl ester **6**, which shows fluorescence induced by conjugation of benzene and imidazole functionalities, were presented and discussed.

Experimental

Reagents and equipments

Melting points were determined on an XT-4B micro melting point apparatus without correction. FT-IR (Fourier transform infrared spectroscopy) spectra were recorded with KBr pellets on a Bruker EQUINOX-55 FT-IR spectrometer. ^{1}H and ^{13}C NMR spectra were recorded on a Varian INOVA-400 spectrometer at 400 and 100 MHz, respectively. Chemical shifts were reported relative to internal standard Me_4Si. Electron spray ionization-mass spectrometry (ESI-MS) analyses were carried out in positive ion modes using a Thermo Finnigan LCQ Advantage MAX LC/MS/MS. The X-ray diffraction data were collected on a Bruker Smart APEX II CCD diffractometer. The X-ray powder diffraction (PXRD) pattern was recorded with a Pigaku D/Max 3III diffractometer. The fluorescent spectrum was measured with a Hitachi F-4500 FL spectrophotometer. The luminescent lifetime was performed on Edinburge FLS920.

And all the reagents and solvents used for synthesis were commercially available and without further purification unless otherwise noted. The reaction process was monitored by thin-layer chromatography (TLC). The products were purified by recrystallization or column chromatography, and the latter was carried out on silica gel (200-300 mesh).

1-(2-Chloroethoxy)-2-nitrobenzene **1**

1-Bromo-2-chloroethane (4.30 g, 0.03mol) and K_2CO_3 (2.07 g, 0.015 mol) were added to a solution of 2-nitrophenol (1.39 g, 0.01mol) in DMF (8 mL) at room temperature, the reaction was kept at 120 °C for 5 h, cooled and diluted with EtOAc (20 mL), then washed with water (3 × 10 mL). The organic layer was collected and concentrated under vacuum, recrystallized in MeOH to give light yellow solid **1**. Yield 93%; m. p. 36-37 °C; ^{1}H NMR ($CDCl_3$, 400 MHz) δ 7.85 (m, 1H), 7.56 (m, 1H), 7.10 (m,

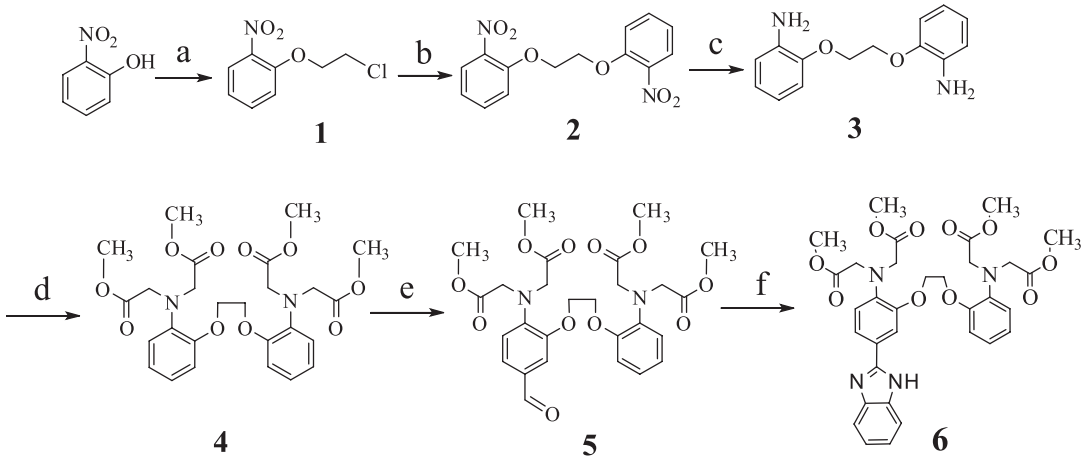

Scheme 1. Synthesis of **6**. Reagents and conditions: (a) $BrCH_2CH_2Cl$, K_2CO_3, DMF, 120 °C, 5 h; (b) 2-NO_2-Ph-OH, K_2CO_3, DMF, 140-160 °C, 4-5 h; (c) Fe, HCl, EtOH, reflux, 4 h; (d) (*i*-Pr)$_2$NEt, $BrCH_2COOCH_3$, MeCN, reflux, 24-36 h; (e) $POCl_3$, DMF, 75 °C, 4 h; (f) 1,2-Ph$(NH_2)_2$, H_2O_2, $Fe(NO_3)_3$, 50 °C, 30 min.

2H), 4.40 (t, 2H, *J* 12 Hz), 3.86 (t, 2H, *J* 12 Hz); IR ν/cm^{-1} 2926, 2875, 1608, 1522, 1343, 1276, 1026, 745, 667.

1-Nitro-2-[2-(2-nitrophenoxy)ethoxy]benzene **2**

To a solution of **1** (2.01 g, 0.01 mol) in DMF (10 mL) at room temperature, 2-nitrophenol (1.39 g, 0.01 mol) and K_2CO_3 (2.50 g, 0.018 mol) were added. The reaction mixture was stirred at 140 °C for 4 h, cooled and poured into cold water (20 mL). The formed yellow solid was filtered and washed with water (3 × 5 mL). The crude product was recrystallized in MeOH to give yellow solid **2**. Yield 95%; m.p. 168-169 °C; ^{1}H NMR ($CDCl_3$, 400 MHz) δ 7.83 (d, 2H, *J* 8 Hz), 7.57 (t, 2H, *J* 8 Hz), 7.24 (t, 2H, *J* 8 Hz), 7.08 (t, 2H, *J* 8 Hz), 4.54 (s, 4H); IR ν/cm^{-1} 3051, 2956, 2931, 1606, 1582, 1518, 1359, 1278, 1159, 1090, 744, 671.

2-[2-(2-Aminophenoxy)ethoxy]benzenamine **3**

Iron powder (3.36 g, 0.06 mol), concentrated hydrochloric acid (0.2 mL), and anhydrous ethanol (10 mL) were added into a dried three-necked flask equipped with a magnetic stirrer. When the mixture was heated to boiling, **2** (3.04 g, 0.01mol) was added in three portions. The mixture was refluxed for 4 h, and then made alkaline to litmus by addition of 15% alcoholic potassium hydroxide solution, the iron powder was removed by filtration afterwards. Into the filtrate, 6 mol L^{-1} sulfuric acid was added and white precipitate was obtained. After filtration, the precipitate was dissolved in 40 mL of warm water and made alkaline to pH = 8 with saturated sodium hydroxide solution. The generated light yellow solid was collected and recrystallized in MeOH to give white solid **3**. Yield 88%; m.p. 116-117 °C; ^{1}H NMR ($CDCl_3$, 400 MHz) δ 6.98 (m, 8H), 4.36 (s, 4H), 3.82 (s, 4H); IR ν/cm^{-1} 3432, 3355, 3059, 2934, 1612, 1507, 1461, 1276, 1217, 941, 739.

1,2-Bis(2-aminophenoxy)ethyl-*N,N,N',N'*-acetic acid methyl ester **4**

Compound **3** (2.44 g, 0.01 mol) was dissolved in MeCN (10 mL), then (*i*-Pr)$_2$NEt (6 mL) and methyl bromoacetate (3 mL) were added to the mixture with stirring. The reaction mixture was refluxed for 24 h. After the reaction, the mixture was cooled down, poured into EtOAc (20 mL), and filtered to remove the generated white solid. The combined EtOAc filtrates were concentrated *in vacuo* to give an oily solid, then adding a little methanol, white solid was generated, filtered, air dried and recrystallized in MeOH to give white solid **4**. Yield 87%; m.p. 94-95 °C; ^{1}H NMR ($CDCl_3$, 400 MHz) δ 6.85 (m, 8H), 4.27 (s, 4H), 4.15 (s, 8H), 3.56 (s, 12H); IR ν/cm^{-1} 3067, 2993, 2951, 2921, 2888, 1748, 1596, 1509, 1173, 742, 706.

[(2-{2-[2-(Bis-methoxycarbonylmethylamino)-5-methylphenoxy]ethoxy}-4-formyl-5-methyl-phenyl) methoxycarbonylmethylamino]acetic acid methyl ester **5**

$POCl_3$ (2.4 mL) was added dropwise over 40-45 min into a dry three-necked flask which contained anhydrous DMF (20 mL). The $POCl_3$/DMF mixture was stirred at room temperature for 1-2 h and added dropwise into a DMF (20 mL) solution of compound **4** (5.32 g, 0.01mol) afterwards. The reaction mixture was heated at 75 °C for 4 h, concentrated *in vacuo*, and then poured into ice water. The suspension was filtered and purified by column chromatography (silica gel, *V*(EtOAc):*V*(hexane) = 1:1 as eluent) to afford white solid **5**.[20] Yield 85%; m.p. 131-132 °C; ^{1}H NMR ($CDCl_3$, 400 MHz) δ 9.80 (s, 1H), 7.38 (m, 2H), 6.86 (m, 4H), 6.76 (d, 1H, *J* 8.3 Hz), 4.31 (m, 2H), 4.27 (m, 2H), 4.24 (s, 4H), 4.15 (s, 4H), 3.57 (s, 6H), 3.56 (s, 6H); ^{13}C NMR ($CDCl_3$, 101 MHz) δ 190.5, 171.9, 171.2, 150.1, 149.6, 145.0, 139.3, 129.9, 126.7, 122.2, 121.6, 116.5, 112.9, 110.5, 77.3, 77.0, 76.7, 67.3, 66.6, 53.4, 53.2, 52.0, 51.9, 51.6; IR ν/cm^{-1} 3015, 2954, 2928, 1746, 1681, 1593, 1509, 1245, 1164, 747; HRMS calcd. for $C_{27}H_{32}N_2O_{11}$: 560.2006, $(M+Na)^+$ calcd.: 583.1898, $(M+Na)^+$ found: 583.1894.

[(2-{2-[2-(Bis-methoxycarbonylmethylamino)phenoxy] ethoxy}-4-benzimidazole-phenyl)methoxycarbonyl-methylamino]acetic acid methyl ester **6**

A mixture of 1,2-phenylenediamine (0.11 g, 1 mmol), compound **5** (0.56 g, 1 mmol), H_2O_2 (30%, 4 mmol, 0.4 mL) and $Fe(NO_3)_3 \cdot 9\,H_2O$ (0.04 g, 0.1 mmol) was heated at 50 °C for 30 min. After completion of the reaction, the reaction mixture was dissolved in EtOH (10 mL) and then poured into ice-water (30 mL). The pure solid product was filtered, washed with ice-water, dried and subsequently purified by column chromatography (silica gel, *V*(EtOAc):*V*(hexane) = 1:1 as eluent)[21,22] to afford white solid **6**. Yield 80%; m.p. 72-73 °C; IR (KBr, cm^{-1}) 3505 (ν_{N-H}), 3033 ($\nu_{=C-H}$), 2906 (ν_{C-H}), 1743 ($\nu_{C=O}$), 1509 ($\nu_{C=C}$), 1478 ($\nu_{C=C}$), 1170 (ν_{C-O}), 746 ($\delta_{=C-H}$); ^{1}H NMR (400 MHz, $CDCl_3$) δ 7.68 (d, 1H, *J* 8 Hz), 7.56 (s, 3H), 7.17 (s, 2H), 6.87 (m, 2H), 6.83 (m, 1H), 6.70 (m, 2H), 4.13 (s, 8H), 3.91 (m, 3H), 3.85 (s, 2H), 3.54 (s, 6H), 3.51 (s, 6H); ^{13}C NMR (100 MHz, $CDCl_3$) δ 172.2, 171.7, 152.2, 150.2, 149.9, 140.8, 138.7, 122.4, 121.4, 120.3, 118.9, 118.2, 112.8, 111.3, 77.4, 77.1, 76.8, 66.9, 66.5, 53.4, 53.3, 51.8; HRMS calcd. for $C_{33}H_{36}N_4O_{10}$: 648.2431, $(M+H)^+$ calcd.: 649.2504, $(M+H)^+$ found: 649.2487.

Single crystals of **6** for X-ray diffraction experiments were obtained from ethyl acetate-dichloromethane mixture (3:1).

Crystal structure determination of [(2-{2-[2-(bis-methoxycarbonylmethylamino)phenoxy]ethoxy}-4-benzimidazole-phenyl)methoxycarbonylmethylamino]acetic acid methyl ester **6**

A colorless crystal with a size of 0.30 × 0.24 × 0.19 mm^3 was selected for X-ray data collection. The X-ray diffraction measurement was made on a Bruker Smart APEX II CCD diffractometer with graphite monochromated Mo-*K*α radiation (λ = 0.71073 Å). The crystal data was collected at room temperature using ω-2θ scan technique. The structure was solved by direct methods with SHELXS-97[23] and refined using SHELXL-97.[24] The crystal data collection and refinement parameters are given in Table 1.

Table 1. Crystallographic data and structure refinement parameters for **6**

Empirical formula	$C_{33}H_{35}N_4O_{10}$
Formula weight	647.65
Temperature / K	296(2)
Wavelength / Å	0.71073
Crystal system	monoclinic
Space group	*C*2/*c*
Unit cell dimension / Å	
A	35.648(3)
B	14.3240(12)
C	15.3693(13)
Volume / Å^3	7820.1(11)
Z	8
Calculated density / (mg m^{-3})	1.100
Absorption coefficient / mm^{-1}	0.082
F(000)	2728
Crystal size / mm^3	0.30 × 0.24 × 0.19
θ range for data collection	1.53-25.10
Limiting indices *h, k, l*	−42/32, −16/17, −16/18
Refinement method	full-matrix least-squares on F^2
Reflections collected/unique/R_{int}	19396/6962/0.0226
Completeness to θ = 25.10°	99.9%
Data/restraints/parameters	6962/0/428
Goodness-of-fit on F^2	1.077
Final *R* índices [$I > 2\sigma(I)$]	
R_1	0.0505
wR_2	0.1546
R indices (all data)	
R_1	0.0685
wR_2	0.1658
Largest diff. peak and hole / (e Å^{-3})	0.497 and −0.220

Results and discussion

Structural characterization

The structure of **6** was characterized by IR, ESI-HRMS, PXRD, ^{1}H and ^{13}C NMR. IR spectrum of **6** shows typical secondary amine absorption (ν_{N-H} 3506 cm^{-1}), aromatic absorption ($\nu_{=C-H}$ 3033 cm^{-1}; $\nu_{C=C}$ 1510, 1478 cm^{-1}; $\delta_{=C-H}$ 746 cm^{-1}) and ester absorption ($\nu_{C=O}$ 1743 cm^{-1}; ν_{C-O} 1171 cm^{-1}). The HRMS *m/z* value, ^{1}H and ^{13}C NMR chemical shifts are in accordance with the structure of **6**. And powder X-ray diffraction at room temperature was carried out to testify the phase purity of assynthesized samples, the diffraction peaks of both simulated[25,26] and experimental patterns match in the key positions, indicating the pure phase of **6**. PXRD pattern of **6** at room temperature can be found in Figure 2.

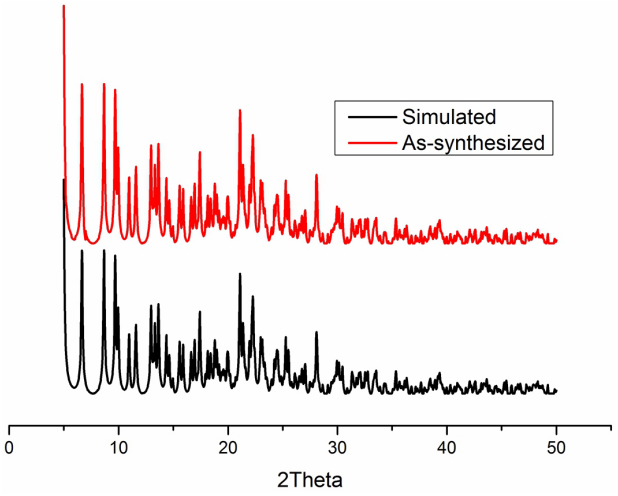

Figure 2. PXRD pattern of **6** at room temperature.

Crystal structure

The molecular structure and atom numbering of **6** are shown in Figure 3, and the crystal packing of **6** along the *c* axis is presented in Figure 4.

The supramolecular packing is determined mainly by the hydrogen bonds C–H···O (Table 2). Due to the intramolecular hydrogen bonds from carboxylic oxygen atoms O4, O7, O9 and ether oxygen atoms O1, O2, microporous skeleton along the *c* axis is formed. And the intermolecular hydrogen bonds between carbonyl oxygen atoms O4 and O9 from a neighboring molecule are observed to extend supramolecular organic frameworks.[27,28]

The investigated compound crystallizes in the *C*2/*c* space group with eight molecules *per* unit cell. Table 3 lists some selected bond lengths and torsion angles for **6** to demonstrate the whole molecular skeleton. It can be

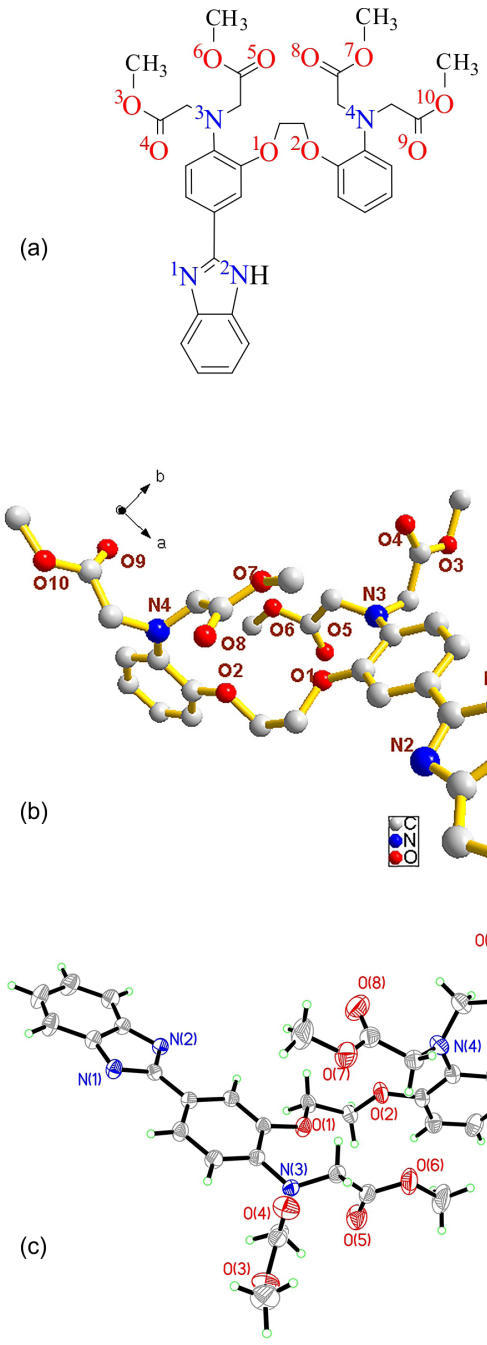

Figure 3. (a) Chemical structural formula, (b) crystal structure and (c) ORTEP diagram (with ellipsoids drawn at the 30% probability level) of **6**.

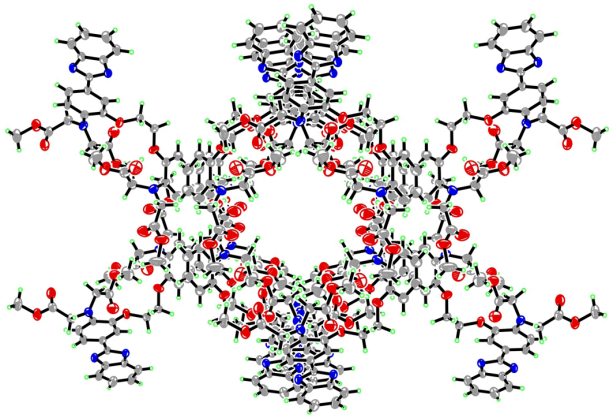

Figure 4. Crystal packing of **6** along the *c* axis.

found that the carbon-carbon bond lengths are basically intermediate between typical C–C single (1.54 Å) and C=C double (1.34 Å) bonds, especially at the connection point of benzene and imidazole (C(7)-C(8) 1.461(3) Å, C(8)-C(13) 1.390(3) Å, C(8)-C(9) 1.394(2) Å, C(9)-C(10) 1.370(3) Å, C(13)-C(12) 1.374(3) Å), and carbon-nitrogen bond lengths are also intermediate between C–N typical single (1.47 Å) and C=N double (1.27 Å) bonds (C(7)-N(1) 1.318(2) Å, C(1)-N(1) 1.386(2) Å, C(6)-N(2) 1.376(2) Å, C(7)-N(2) 1.368(2) Å), the coplanarity of benzene and imidazole can be predicted. Moreover, from the close-to-180° torsion angles N(2)-C(7)-C(8)-C(13) −172.76(17) Å, N(1)-C(7)-C(8)-C(9) −173.77(17) Å, N(2)-C(6)-C(1)-C(2) −179.52(18) Å, C(5)-C(6)-C(1)-N(1) 178.67(18) Å, molecular planarity can be further confirmed. The coplanarity adopted for benzene and imidazole enables delocalized electrons transfer and enhances the fluorescence.

In one molecule, due to the flexible ether bonding, the two benzene rings are in an almost perpendicular configuration with a close-to-90° angle of 86.44°, which can be calculated by means of plane angles through the model of dihedral angles. The tertiary amino group is distorted from planarity of phenyl ring, and the four straight chains of acetic acid methyl ester, which are connected to nitrogen

Table 2. Geometry of the C–H···O hydrogen bonds in the crystals of **6**

D–H···O	d(D–H) / Å	d(H···O) / Å	d(D···O) / Å	∠(DHO) / degree
Intra C(22)–H(22A)···O(9)	0.97	2.60	3.197(3)	120
Intra C(22)–H(22B)···O(2)	0.97	2.45	2.800(3)	101
Intra C(28)–H(28A)···O(4)	0.97	2.54	3.131(2)	119
Intra C(28)–H(28B)···O(1)	0.97	2.34	2.746(2)	105
Intra C(28)–H(28B)···O(7)	0.97	2.59	3.529(3)	163
C(4)–H(4)···O(4)[a]	0.93	2.53	3.453(3)	171
C(30)–H(30B)···O(9)[b]	0.96	2.59	3.432(4)	147

Symmetry code: [a]1-x, y, 1/2-z; [b]1/2-x, -1/2+y, -1/2-z.

Table 3. Some selected bond lengths and torsion angles for **6**

Bond length / Å		Torsion angle / degree	
C(7)–N(1)	1.318(2)	C(5)-C(6)-C(1)-N(1)	178.67(18)
C(1)–N(1)	1.386(2)	N(2)-C(6)-C(1)-C(2)	–179.52(18)
C(7)–N(2)	1.368(2)	N(1)-C(7)-C(8)-C(9)	–173.77(17)
C(6)–N(2)	1.376(2)	N(2)-C(7)-C(8)-C(13)	–172.76(17)
C(11)–N(3)	1.403(2)	C(9)-C(10)-O(1)-C(14)	–9.1(3)
C(28)–N(3)	1.441(2)	C(15)-C(14)-O(1)-C(10)	–172.95(15)
C(31)–N(3)	1.434(2)	C(14)-C(15)-O(2)-C(16)	179.83(17)
C(21)–N(4)	1.406(3)	O(1)-C(14)-C(15)-O(2)	–75.54(19)
C(22)–N(4)	1.427(3)	C(17)-C(16)-O(2)-C(15)	–1.5(3)
C(25)–N(4)	1.443(3)	C(12)-C(11)-N(3)-C(31)	23.2(3)
C(1)–C(2)	1.389(3)	C(10)-C(11)-N(3)-C(28)	47.8(3)
C(6)–C(1)	1.391(3)	N(3)-C(28)-C(29)-O(5)	1.3(3)
C(6)–C(5)	1.392(3)	N(3)-C(28)-C(29)-O(6)	–177.59(17)
C(7)–C(8)	1.461(3)	O(4)-C(32)-C(31)-N(3)	–1.2(3)
C(8)–C(9)	1.394(2)	O(3)-C(32)-C(31)-N(3)	179.62(17)
C(8)–C(13)	1.390(3)	C(32)-C(31)-N(3)-C(28)	69.0(2)
C(9)–C(10)	1.370(3)	C(16)-C(21)-N(4)-C(25)	–143.0(2)
C(13)–C(12)	1.374(3)	C(20)-C(21)-N(4)-C(22)	–126.5(2)
C(11)–C(10)	1.407(2)	N(4)-C(22)-C(23)-O(8)	–3.9(4)
C(14)–C(15)	1.494(3)	N(4)-C(22)-C(23)-O(7)	176.39(18)
C(16)–C(17)	1.381(3)	N(4)-C(25)-C(26)-O(9)	1.3(4)
C(21)–C(16)	1.395(3)	N(4)-C(25)-C(26)-O(10)	–178.8(2)
C(17)–C(18)	1.379(3)	C(26)-C(25)-N(4)-C(22)	69.4(3)
C(22)–C(23)	1.498(3)		
C(25)–C(26)	1.503(3)		
C(28)–C(29)	1.500(3)		
C(32)–C(31)	1.502(3)		

atoms in benzene rings, keep certain angles and make the intramolecular hydrogen bonds possible, thus micropores are formed, as indicated clearly by the intramolecular hydrogen bonds from carboxylic oxygen atoms O4, O7, O9 and ether oxygen atoms O1, O2. And the intermolecular hydrogen bonds between carbonyl oxygen atoms O4 and O9 from a neighboring molecule are observed to extend supramolecular organic architecture.

Fluorescent spectrum and luminescent lifetime

The solid state fluorescent spectrum of **6** at room temperature is given in Figure 5. **6** in the solid state displays a blue emission with emission peaks at 389.6 nm and 461.6 nm upon excitation at 310 nm. The emission peak at 389.6 nm can be assigned to π-π^* transitions of benzene and imidazole delocalized π electrons, 461.6 nm emission peak is probably due to n-π^* transitions of n electrons in nitrogen atoms of imidazole.

The luminescent lifetime τ indicates the average time of a molecule at excitation state. A small value of τ, which means the molecule can recover quickly from the excitation state and allow multi-excitations, always comes along with high sensitivity in luminescence. As shown in Figure 6, the decay lifetime curve of **6** can be well fitted with double-exponential decay, giving two lifetimes of $\tau_1 = 0.68$ ns and $\tau_2 = 2.68$ ns ($\chi^2 = 1.252$), which suggest fluorescence.[29]

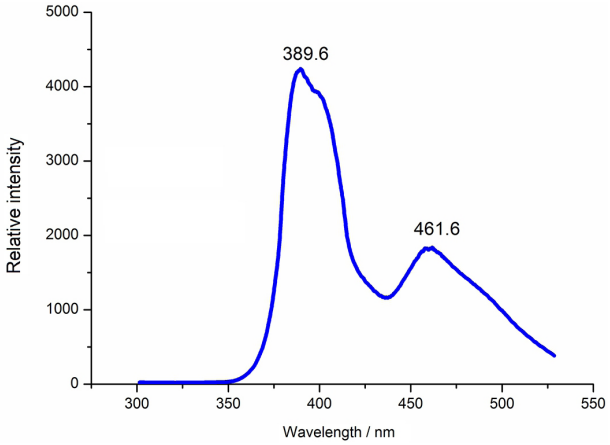

Figure 5. Solid state emission of **6** on excitation at 310 nm.

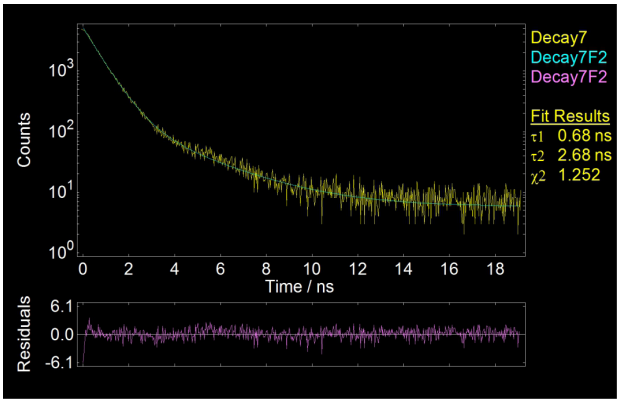

Figure 6. Luminescent lifetime curve of **6** monitored at corresponding excitation/emission maxima, which can be fitted with double-exponential decay, fitting results: $\tau_1 = 0.68$ ns, $\tau_2 = 2.68$ ns ($\chi^2 = 1.252$).

Conclusions

The investigated molecule **6** is fluorescent and has two luminescent lifetimes. Furthermore, single crystal X-ray diffraction study indicates that the electrons are delocalized and inter-, intramolecular hydrogen bonds are displayed in the molecular system. The planarity of molecular skeleton and luminescence make delocalized electrons transfer and migration possible. These characteristics are unique and clearly originate from the highly ordered structure of **6**.

Exploration of functional microporous crystalline materials is a probable way to the development of novel materials. And formation of optoelectronic devices is expected by filling the micropores with photoactive molecules such as electron acceptors in similar crystalline materials of **6**, which worth our attention and will be a target for further investigation.

Supplementary Information

Crystallographic data (excluding structure factors) for the structures in this work were deposited in the Cambridge Crystallographic Data Centre as supplementary publication number CCDC 922862. Copies of the data can be obtained, free of charge, via www.ccdc.cam.ac.uk/conts/retrieving.html or from the Cambridge Crystallographic Data Centre, CCDC, 12 Union Road, Cambridge CB2 1EZ, UK; fax: +44 1223 336033. E-mail: deposit@ccdc.cam.ac.uk.

Acknowledgement

This work was financially supported by the National Natural Science Foundation of China (NSFC-21172178).

References

1. Wang, Q. M.; Shen, D.; Bulow, M.; Lau, M. L.; Deng, S.; Fitch, F. R.; Lemcoff, N. O.; Semanscin, J.; *Microporous Mater.* **2002**, *55*, 217.
2. Ngo, H.; Lin, W.; *Top. Cat.* **2005**, *34*, 85.
3. Rowsell, J. L. C.; Yaghi, O. M.; *Angew. Chem. Int. Ed.* **2005**, *44*, 4670.
4. Weber, J.; Thomas, A.; *J. Am. Chem. Soc.* **2008**, *130*, 6334.
5. Tilford, R. W.; Mugavero III, S. J.; Pellechia, P. J.; Lavigne, J. J.; *Adv. Mater.* **2008**, *20*, 2741.
6. Endo, K.; Koike, T.; Sawaki, T.; Hayashida, O.; Masuda, H.; Aoyama, Y.; *J. Am. Chem. Soc.* **1997**, *119*, 4117.
7. Thallapally, P. K.; McGrail, B. P.; Atwood, J. L.; Gaeta, C.; Tedesco, C.; Neri, P.; *Chem. Mater.* **2007**, *19*, 3355.
8. Tsue, H.; Matsui, K.; Ishibashi, K.; Takahashi, H.; Tokita, S.; Ono, K.; Tamura, R.; *J. Org. Chem.* **2008**, *73*, 7748.
9. Lim, S.; Kim, H.; Selvapalam, N.; Kim, K. J.; Cho, S. J.; Seo, G.; Kim, K.; *Angew. Chem. Int. Ed.* **2008**, *47*, 3352.
10. Berthod, A.; Ruiz-Angel, M.; Carda-Broch, S.; *J. Chromatogr. A* **2008**, *1184*, 6.
11. Marszall, M. P.; Kaliszan, R.; *Crit. Rev. Anal. Chem.* **2007**, *37*, 127.
12. Gross, G. M.; Reid, V. R.; Synovec, R. E.; *Curr. Anal. Chem.* **2005**, *1*, 135.
13. Eiceman, G. A.; Gardea-Torresdey, J.; Overton, E.; Carney, K.; Dorman, F.; *Anal. Chem.* **2004**, *76*, 3387.
14. Klots, T. D.; Devlin, P.; Collier, W. B.; *Spectrochim. Acta Part A* **1997**, *53*, 2445.
15. Morsy, M. A.; *J. Phys. Chem. A* **2002**, *106*, 9196.
16. Yurdakul, S.; Yilmaz, C.; *Vib. Spectrosc.* **1999**, *21*, 127.
17. Liu, T. F.; Wu, W. F.; Wan, C. Q.; He, C. H.; Jiao, C. H.; Cui, G. H.; *J. Coord. Chem.* **2011**, *64*, 975.
18. Krossing, I.; Slattery, J. M.; Daguenet, C.; Dyson, P. J.; Oleinikova, A.; Weingaortner, H.; *J. Am. Chem. Soc.* **2006**, *128*, 13427.
19. Billard, I.; Moutiers, G.; Labet, A.; El Azzi, A.; Gaillard, C.; Mariet, C.; Lutzenkirchen, K.; *Inorg. Chem.* **2003**, *42*, 1726.
20. Wang, J. B.; Qian, X. H.; *Org. Lett.* **2006**, *8*, 3721.
21. Bahrami, K.; Khodaei, M. M.; Naali, F.; *Synlett* **2009**, 569.
22. Yang, H. W.; Yue, F.; Feng, S.; Wang, J. D.; Liu, A. H.; Chen, H. M.; Yu, K. B.; *Chin. Org. Chem.* **2004**, *24*, 792.
23. Sheldrick, G. M.; *SHELXS-97*; *Program for Solution Crystal Structure*; University of Göttingen, Germany, 1997.
24. Sheldrick, G. M.; *SHELXL-97*; *Program for Solution Crystal Structure and Refinement*; University of Göttingen, Germany, 1997.
25. Dinnebier, R. E.; Billinge, S. J. L.; *Powder Diffraction: Theory and Practice*; Royal Society of Chemistry: Cambridge, UK, 2008.
26. Pecharsky, V. K.; Zavalij, P. Y.; *Fundamentals of Powder Diffraction and Structural Characterization of Materials*, 2nd ed.; Springer: Berlin, Germany, 2009.
27. Steiner, T.; *Cryst. Rev.* **1996**, *6*, 1.
28. Jeffrey, G. A.; Maluszynska, H.; Mitra, J.; *Int. J. Biol. Macromol.* **1985**, *7*, 336.
29. Dias, H. V. R.; Diyabalanage, H. V. K.; Eldabaja, M. G.; Elbjeirami, O.; Rawashdeh-Omary, M. A.; Omary, M. A.; *J. Am. Chem. Soc.* **2005**, *127*, 7489.

Submitted: August 25, 2013
Published online: November 26, 2013